Modeling Minimally-processed Arc Weld Transformers for Rural Minigrid Applications

[1]James Cale, [1]Christopher Lute, [1]John Simon, [2]Amanda DelCore

[1]Colorado State University, [2]Factor[e] Ventures

CSU Energy Institute – Powerhouse Energy Campus – Fort Collins, Colorado (USA), 80524

James.Cale,Chris.Lute,John.Simon(@colostate.com), amanda@factore.com

1. Introduction

- Per capita energy usage has been shown to be directly correlated with economic output and literacy rates.[1]
- Enabling worldwide, affordable access to electricity is a goal of many government and philanthropic organizations around the world.
- According to the International Energy Agency (IEA), by the year 2030, 674 million people will be without access to electricity.[2]
- **Minigrids may be able to provide energy access to nearly 300 million additional people (relative to current planning scenarios) by 2030[2], see Fig. 1.**

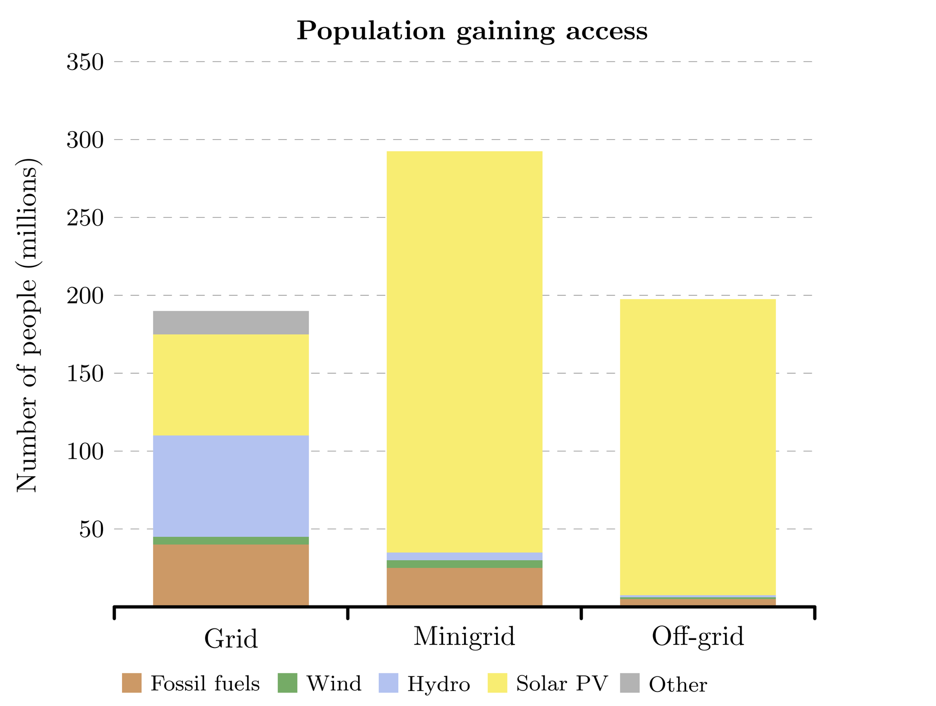

Fig. 1: *Additional population gaining access under Energy For All plan, relative to New Policies Scenario, 2017–2030.*[2]

- Sub-Saharan Africa provides a large opportunity for electrification via minigrids, with a projected 600 million people without electricity by 2030 (mostly in rural areas).

2. Minigrid Design Challenges

- Examples of small commercial businesses in rural microeconomies are: grain milling, refrigeration, barber shops, and welding shops.
- Many of these electrical loads are highly inductive; components may be fabricated by hand and/or specifications may not exist.
- Lack of detailed component specifications makes modeling or designing minigrids difficult (e.g., specifying minigrid controls, generation and storage).

Fig. 2: *Handmade arc welder (Kigali, Rwanda, 2018).*

3. Background on Arc Welding

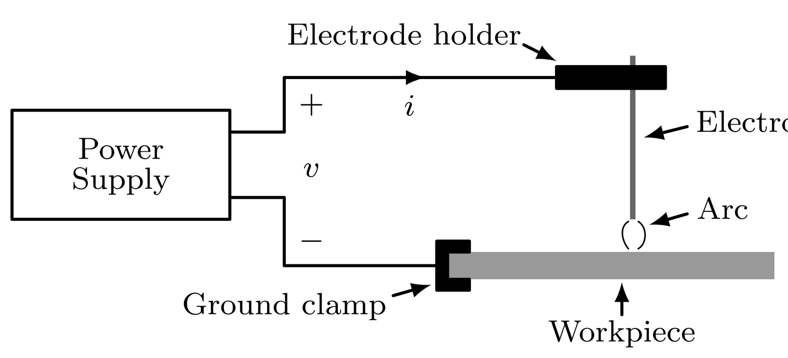

Fig. 3: *Simplified diagram of shielded metal arc welding arrangement.*

- The power supply provides voltage v and current i which establishes electrical arc; current returns through ground clamp.
- Common types are shielded metal arc welding (SMAW), flux-cored, and gas metal arc welding.
- Commercial arc weld power supplies use power electronic converters to regulate current regardless of arc length.
- SMAW is a less-expensive type of welding; the arc is established and maintained manually and uses consumable electrodes.
- The power supply in *transformer-style* SMAW is a single-phase, step-down transformer connected to AC voltage source.

Objective: develop and validate a detailed electromagnetic model for accurate prediction of load current in transformer-style SMAW applications.

4. Model for Transformer-style SWAM

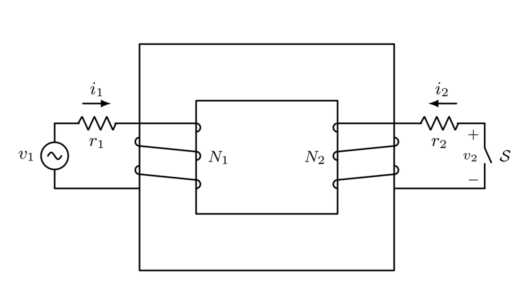

Fig. 4: *Simplified diagram of transformer-style SMAW.*

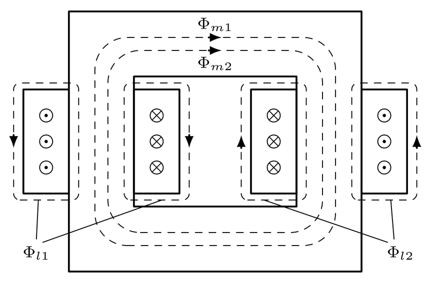

Fig. 5: *Magnetic fluxes in transformer of Fig. 4.*

$$v_1 = r_1 i_1 + \frac{d\lambda_1}{dt} \qquad v_2 = r_2 i_2 + \frac{d\lambda_2}{dt}$$

$$\begin{aligned}\lambda_1 &= N_1(\Phi_{\ell 1} + \Phi_{m1} + \Phi_{m2}) \\ &= \lambda_{\ell 1} + \lambda_{m11} + \lambda_{m12} \\ \lambda_2 &= N_2(\Phi_{\ell 2} + \Phi_{m2} + \Phi_{m1}) \\ &= \lambda_{\ell 2} + \lambda_{m22} + \lambda_{m21}\end{aligned}$$

5. Coupled Nonlinear Electromagnetic System

Calculating Anhysteretic Fluxes and Field Intensity

$$\Phi_m = \int \mathbf{B} \cdot d\mathbf{A} \qquad \mathbf{B} = \mu_0(\mathbf{H} + \mathbf{M})$$

$$B_{an}(H) = \mu(|H|)H$$

$$\oint_{l_p} \mathbf{H} \cdot d\boldsymbol{\ell} = i_{enc} \qquad M_{an} = (\mu(|H|)/\mu_0 - 1)\, H$$

$$H = \left(\frac{1}{l_p}\right)\sum_n N_n i_n = \left(\frac{1}{l_p}\right)(N_1 i_1 + N_2 i_2)$$

Voltage from Magnetizing Flux Linkage

$$\begin{aligned}\frac{d}{dt}\lambda_{mn} &= N_n A_c \frac{d}{dt} B_{an}(H) \\ &= N_n A_c \left(\frac{\partial}{\partial H}\mu(|H|)|H| + H\right)\frac{dH}{dt}\end{aligned}$$

Coupled Nonlinear State Equations

$$\frac{d}{dt}\begin{bmatrix} H_1 \\ H_2 \end{bmatrix} = \begin{bmatrix} \alpha_{11}(H) & \alpha_{12}(H) \\ \alpha_{21}(H) & \alpha_{22}(H) \end{bmatrix}\begin{bmatrix} H_1 \\ H_2 \end{bmatrix} + \begin{bmatrix} \beta_{11}(H) \\ \beta_{12}(H) \end{bmatrix} v_1$$

$$\begin{aligned}f(H) &:= \frac{\partial}{\partial H}\mu(|H|)|H| + H \\ \gamma_1(H) &:= l_{\ell 1}(N_1/l_p) + N_1 A_c f(H) \\ \gamma_2(H) &:= l_{\ell 2}(N_2/l_p) + N_2 A_c f(H) \\ g(H) &:= \gamma_1(H)\gamma_2(H) - N_1 N_2 A_c^2 f^2(H)\end{aligned}$$

$$\begin{aligned}\alpha_{11}(H) &= \gamma_2(H) r_1 (N_1/l_p)/g(H) \\ \alpha_{12}(H) &= N_1 A_c (z + r_2) f(H)/g(H) \\ \alpha_{21}(H) &= -\gamma_1(H)(z + r_2)(N_2/l_p)/g(H) \\ \alpha_{22}(H) &= N_2 A_c r_1 f(H)(N_1/l_p)/g(H) \\ \beta_{11}(H) &= \gamma_2(H)/g(H) \\ \beta_{12}(H) &= -N_2 A_c f(H)/g(H)\end{aligned}$$

6. Magnetic Parameter Identification

$$\begin{aligned}M(t) = &\frac{1}{\mu_0 N_1 A_c}\left(\left(\int_0^T (v_1(\tau) - r_1 i_1(\tau))\, d\tau + \lambda_1(0)\right)\right. \\ &- \frac{1}{\mu_0 N_1 A_c}\left(L_{\ell 1} + \mu_0 A_c N_1^2/l_p\right) i_1(t)\end{aligned}$$

$$M_{an}(H) = \mathrm{sgn}(H)\sum_{k=1}^{K}\frac{m_k(|H|/b_k)^{n_k}}{1 + m_k(|H|/b_k)^{n_k}}$$

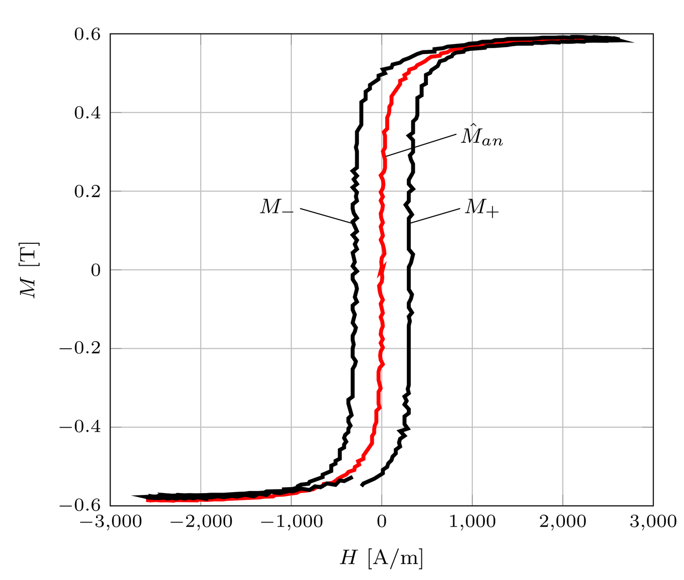

Fig. 6: *Major hysteresis loop (black); anhysteretic (red).*

Optimization (Unconstrained Maximization)

Design Candidate: $\boldsymbol{\theta} = [m_1 \ldots m_K \,|\, b_1 \ldots b_K \,|\, n_1 \ldots n_K]$

$$\max_{\boldsymbol{\theta}} f(\boldsymbol{\theta}) := \frac{1}{||M_{an}(\hat{H}^n_{an}; \boldsymbol{\theta}) - \hat{M}^n_{an}(\hat{H}^n_{an})||_2 + \epsilon}, \; \forall n \in \mathcal{N}$$

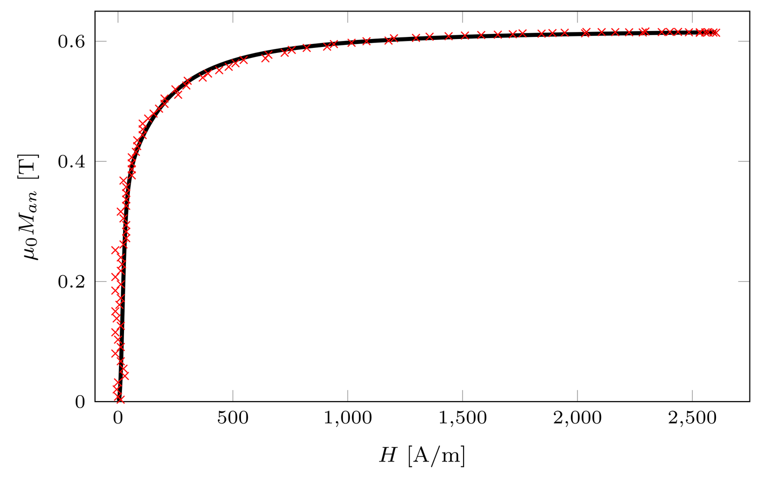

Fig. 7: *Fitted anhysteretic magnetization (black line) versus estimated anhysteretic magnetization samples (red x's).*

Table 1: *Optimized magnetization parameters.*

Param.	Value	Param.	Value	Param.	Value
m_1	2.11×10^5	b_1	1.82×10^2	n_1	1.34
m_2	2.84×10^5	b_2	2.27×10^3	n_2	3.22

7. Model Validation

Fig. 8: *Welding experiment (CSU Powerhouse, 2018).*

- Live arc welding experiments were performed using the SMAW transformer at CSU Powerhouse Energy Campus.
- Primary and secondary currents and voltages during welding experiments were measured (7.68 kS/s).
- Low voltage measurements (in magnetically linear region) were also collected (20 kS/s).

Simulation vs. Experimental Measurements

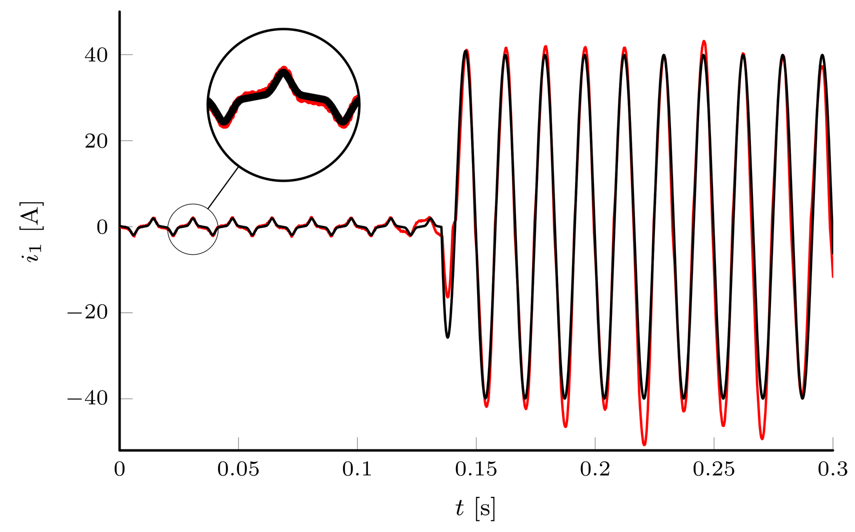

Fig. 9: *Simulated (red) vs. measured (black) current.*

8. Conclusions and Future Work

- A detailed nonlinear electromagnetic model was developed and validated for simulated transformer-style SWAM.
- Simulations were shown to agree well with arc weld measurements, although intermittent current spikes were observed.
- Future work will consider nonlinear arc impedance, temperature effects, and additional transformer types and geometries.

References

[1] R. Cabraal, D.F. Barnes, and S.G. Agarwal "Productive Uses of Energy for Rural Development," *Annual Review of Environment and Resources*, vol. 30, no. 1, pp. 117–144, 2005.

[2] International Energy Agency. *Energy Access Outlook 2017: From Poverty to Prosperity*, World Energy Outlook Special Report, 2017.

[3] J. Cale, S. D. Sudhoff, and J. Turner, "An improved magnetic characterization method for highly permeable materials," *IEEE Transactions on Magnetics*, vol. 42, no. 8, pp. 19741981, 2006.